Journal of Research and Applications in Mechanical Engineering
ISSN: 2229-2152 (Print); 2697-424x (Online)
(2020) Vol. 8, No. 1, 11-21
DOI: 10.14456/jrame.2020.2


*Research Article*

# THERMAL INVESTIGATION OF CELL ARRANGEMENTS FOR CYLINDRICAL BATTERY WITH FORCED AIR-COOLING STRATEGY

**W. Intano**[1]
**A. Kaewpradap**[1]
**S. Hirai**[2]
**M. Masomtob**[3,*]
[1] *Department of Mechanical Engineering, King Mongkut's University of Technology Thonburi, Bangkok, 10140, Thailand*
[2] *Department of Mechanical Engineering, Tokyo Institute of Technology, Tokyo, Japan*
[3] *Materials for Energy Research Unit, National Metal and Materials Technology Center (MTEC), National Science and Technology Development Agency (NSTDA), Pathum Thani, 12120, Thailand*

**Received** 7 July 2019
**Revised** 20 November 2019
**Accepted** 22 November 2019

**ABSTRACT:**
*The cell arrangement is one of the most crucial rules for designing an efficient cooling system of the lithium-ion battery pack in electric vehicles (EVs). This study focused on the decreasing of the temperature of the battery pack with simple arrangements that utilized the space and the turbulent airflow passing the battery pack was considered. Furthermore, this paper aims to comparative analysis of different arrangements (aligned, staggered) with an increasing number of columns and adjusting the gaps between the cells to reduce the temperature of the battery. Parametric analysis effected on the cooling performance is studied on a cylindrical battery pack with a forced air-cooling system in axial-flow configuration based on computational fluid dynamics (CFD). The results showed that the increase in the number of columns leads to reduce the air velocity and lower the heat dissipation of the battery. Furthermore, the aligned arrangement has the best cooling performance. After adjusting the gaps between the center of battery cells found that the temperature decreased by increase the gaps between cells due to the gaps lead to improve the turbulent flow which was larger heat transfer and the gap at 13 mm is the best option in this study.*

**Keywords:** *Battery pack, Battery thermal management, Computational fluid dynamics and Air-cooling strategy*

## 1. INTRODUCTION

Electric vehicles (EVs) have become a part to reduce emissions and the battery is the main source of energy use to drive an electric vehicle. At present, the lithium-ion battery is one of the choices for alternative energy in vehicle power systems because of its high specific energy and no memory effect. However, the performance (e.g., the cycle life, discharge capacity, safety, etc.) of lithium-ion batteries is greatly affected by the operating temperature. The previous studies have shown that the temperature of the battery at 15–40 °C is a suitable operating temperature [1].

Many recent studies have investigated the design of different arrangements of the battery cell that could be operated in the suitable temperature, Yang et al. [2] studied the effects of longitudinal and transverse spacing on the cooling performances of the aligned and the staggered arrays for the battery pack. Changwei et al. [3] adjust the interval between each cell to improve its uniformity. Although, researchers devoted to the design of cell arrangement for the battery pack, but a few researchers involved investigation of air flows with the design of battery arrangements for a cylindrical battery pack.

* Corresponding author: M. Masomtob
E-mail address: manopm@mtec.or.th

The flow through the battery arrangements is the same concept of the flow through the tube bank. The two most common geometric arrangements of a tube bank are aligned and staggered. In any of the arrangements have the diameter of tube (D), the longitudinal spacing ($S_L$) and the transverse spacing ($S_T$). The variation of heat transfer around a tube bank is determined by the flow pattern, which greatly depends on the arrangement of the tubes bank. Moreover, the heat transfer for any particular tube thus not only determined by the incident fluid conditions but also by D, $S_L$, and $S_T$ and the tube positions in the bank [4]. Žukauskas [5] found that tube banks of both arrangements a higher turbulence intensity in the flow causes an increase in the heat transfer at the front as well as the rear portions of a tube. Haider et al. [6] studied heat transfer and flow characteristics past a single cylinder, inline array and staggered array at various Reynolds numbers. The results found that the staggered arrangement gives higher heat transfer rates than the in-line arrangement. Yoo et al. [7] Investigated the heat transfer characteristics of staggered tube banks for various tube spacings, tube locations. The results found that the local heat transfer coefficients on each tube increase except on the front part of the first tube as the tube spacing decreases. Furthermore, the battery pack depends on the pattern of the structural connection when design the battery pack should be considered about space utilization.

At present, the cylinder shape for the battery housing is a controversial issue regarding effective space utilization. It depended on the pattern of the structural connection. Fan et al. [8] calculate the space utilization for the battery packs arrayed in an aligned and staggered arrangement. This study was found that both arrangements were quite closed to each other for space utilizations. Besides, space utilization depends on the diameter and the number of batteries, but not on the length of the batteries [9]. Whenever there were not too many batteries in the battery pack, which a 90° connection in a battery pack was better for space utilization. However, the width of the battery pack is narrower when a 60° connection was applied. The space utilization of the 60° connection is preferable to the 90° connection when there are more batteries in the battery pack. In theory, the space utilization of the 90° connection is better than that of the 60° connection. However, for practical applications, the free space inside the battery pack could not be easily accessed manually or even with standard tools when the 90° connection is used. Therefore, this paper aims to reduce the temperature of the battery pack by a simple arrangement that considers the space utilization of the battery pack.

This study will focus on the improvement of airflow with the turbulent flow by adjusting the gap between the cells from the center to the center of other cells in a vertical direction, thereby reducing temperature inconsistency. Different arrangements and the number of columns for battery cells are compared in this paper. Moreover, this article also studied about the increasing number of columns for battery cell how effects on the temperature of the battery pack when using 90° and 60° connection. Parametric analysis is studied on a cylindrical battery pack with the forced air-cooling system in axial-flow configuration based on computational fluid dynamics (CFD).

## 2. HEAT GENERATION MODEL AND PARAMETERS STUDY

The schematic diagram of the model is shown in Fig. 1. The cylindrical battery cell is used in this module, and the theoretical capacity of the battery is 0.5C (1.3 Ah). The 2D model of battery is developed on CFD software ANSYS Fluent. The heat generation of each cell is obtained by the experiment model [10]. The design parameters are shown in Table 1. Therefore, it is necessary to establish heat source models to simulate the state of all cells in battery pack.

**Table 1:** Design parameters of the battery arrangements.

| Parameter | Aligned | Staggered |
|---|---|---|
| Longitudinal gap, *D* | 18 mm | 18 mm |
| Transverse gap, *L* | 20 mm | 20 mm |

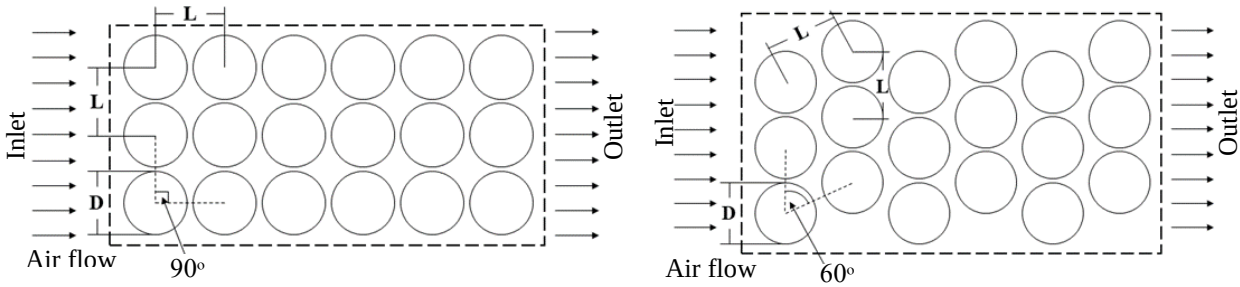


(a) Aligned arrangement (b) Staggered arrangement

**Fig. 1.** The schematic diagram of battery pack model.

*2.1 Heat generation source*

The heat generation inside of battery is joule heating and heat generation due to entropy change that considered as heat generation sources of a battery. The heat generation equation of the battery is shown as follows:

$$\dot{Q}_{battery} = \dot{Q}_{Joule} + \dot{Q}_{entropy} \quad (1)$$

*2.1.1 Joule heating*

Joule heating is the consequence of electric loss in the form of heat, which can be seen in the form of a decrease in voltage due to internal resistance ($R_{\text{int}}$) described as

$$\dot{Q}_{Joule} = I^2 R_{int} \quad (2)$$

The internal resistance ($R_{\text{int}}$) as in Eq. (2) consist of three terms: diffusion resistance caused by the concentration gradient in electrolyte when reaction is performed, ion transport resistance caused by the movement of ions and Ohmic resistance which is caused by the electrodes and internal component materials [11].

*2.1.2 Heat generation due to entropy change*

The other heat generation comes from the change of entropy. When the battery is discharged and performs chemical reaction, some of energy carries out the electricity. The rest becomes the loss in term of heat which can be detected as the change of entropy expressed by:

$$\dot{Q}_{entropy} = -T\Delta S(\frac{I}{nF}) \quad (3)$$

According to Chanthevee P et al. [10], have experiment about the heat generation of single Lithium Cobalt Oxide battery cell (LCO) at the ambient temperature as 25 °C. The load is applied at 0.5C discharge rate (1.3A), the continuous discharge recommended from the specifications of the battery. The heat generation is shown in Table 2 as below:

**Table 2:** Joule heating and heat generation due to entropy change at 0.5C discharge rate (1.3A).

| **Time, s** | $\dot{Q}_{joule}$ **, W** | $\dot{Q}_{entropy}$**, W** |
|---|---|---|
| 0 | 0.0920 | 0.045 |
| 720 | 0.0924 | 0.050 |
| 1440 | 0.0925 | 0.155 |
| 2160 | 0.0927 | 0.165 |
| 2880 | 0.0932 | 0.180 |
| 3600 | 0.0938 | 0.180 |
| 4320 | 0.0947 | 0.180 |
| 5040 | 0.0956 | 0.180 |
| 5760 | 0.0967 | 0.255 |
| 6480 | 0.0988 | 0.305 |
| 6600 | 0.0993 | 0.330 |

*2.2 Numerical modeling*

For the air flow passing through the battery pack, the governing equations used in the simulation are expressed in Equations 4 to 8 [12-13].

*2.2.1 Continuity equation*

$$\nabla \vec{v} = 0 \tag{4}$$

*2.2.2 Momentum conservation equation*

$$\frac{\partial \vec{v}}{\partial t} + (\vec{v}\nabla)\vec{v} = -\frac{\nabla p}{\rho} + \frac{\mu}{\rho}\nabla^2 \vec{v} \tag{5}$$

*2.2.3 Energy conservation equation*

$$\rho c_p \left(\frac{\partial E}{\partial t} + v_x \frac{\partial E}{\partial x} + v_y \frac{\partial E}{\partial y} + v_z \frac{\partial E}{\partial z}\right) = k_T \left(\frac{\partial^2 E}{\partial x^2} + \frac{\partial^2 E}{\partial y^2} + \frac{\partial^2 E}{\partial z^2}\right) \tag{6}$$

*2.2.4 Turbulent kinetic energy equation*

$$\rho_a u_j \frac{\partial k}{\partial x_j} = \frac{\partial}{\partial x_j}\left[\left(\mu + \frac{\mu_t}{\sigma_k}\right)\frac{\partial k}{\partial x_j}\right] + \frac{\mu_t}{2}\left(\frac{\partial u_i}{\partial x_j} + \frac{\partial u_j}{\partial x_i}\right)^2 - \rho_a \varepsilon \tag{7}$$

*2.2.5 Turbulent kinetic energy dissipation rate equation*

$$\rho_a u_j \frac{\partial \varepsilon}{\partial x_j} = \frac{\partial}{\partial x_j}\left[\left(\mu + \frac{\mu_t}{\sigma_\varepsilon}\right)\frac{\partial \varepsilon}{\partial x_j}\right] + C_1 \frac{\mu_t}{2}\left(\frac{\partial u_i}{\partial x_j} + \frac{\partial u_j}{\partial x_i}\right)^2 \frac{\varepsilon}{k} - C_2 \rho_a \frac{\varepsilon^2}{k} \tag{8}$$

The viscosity of turbulence flow, $\mu_t$ is calculated by combination of k and ε as follow:

$$\mu_t = \rho C_\mu \frac{k^2}{\varepsilon} \tag{9}$$

Where k and ε are the turbulent kinetic energy and the turbulent kinetic energy dissipation rate, respectively. $u_i$ and $u_j$ are the averaged velocity components. $p$ and $\rho_a$ are the average pressure and the density of air. $\mu$ is the molecular dynamic viscosity coefficient, $\mu_t$ is the turbulent dynamic viscosity coefficient. $C_\mu$, $\sigma_k$, $\sigma_\varepsilon$, $\sigma_T$ are the constant parameters of the k-ε turbulence model. In these equations, the typical constant values of the parameters in k-ε model are given by the following values:

$C_1$ = 1.44, $C_2$ = 1.92, $C_\mu$ = 0.09, $\sigma_k$ = 1, $\sigma_\varepsilon$= 1.3, $\sigma_T$ = 0.85

The set of governing equations was solved by using ANSYS Fluent which is based on the finite volume method. In the CFD analysis, the buoyancy effect of air was neglected; based on the Reynolds number, under the case of natural convection cooling, turbulence model was selected and under the case of forced air cooling strategy, the k-ε turbulence model is used to calculate the turbulence flow; using difference scheme of second-order upstream, the Navier–Stokes momentum equation was solved.

*2.3 Parameters study*

This study will use the heat source based on experimental data by Chanthevee P et al. [10] which collect the data from experiment of single battery cell. The heat generation will apply to the cylindrical battery cell in simulation software. For parameters that study is shown as Table 3.

**Table 3:** Model parameters for the battery pack.

| Experimental parameter | Parametric study |
|---|---|
| Battery arrangement | Aligned (90°), Staggered (60°) |
| Gap between cells, Y | 10, 11, 12, 13 mm |
| Number of columns | 6, 7, 8, 9 |
| Discharge rate, C-rate | 0.5 C |
| Air inlet temperature, $T_i$ | 25 °C |
| Air mass flow rate, $\dot{m}_a$ | 0.0175 kg/s |

## 3. SIMULATION SETUP

In this study, a 2D battery pack model is solved by the commercial computation fluid dynamic software ANSYS Fluent. A turbulent k-ε model is employed to acquire the flow field of cooling air between cells.

### *3.1 Assumption*

This work will reduce many complications of the simulation. A few parts in the battery module are not considered such as the insulator between battery cells, small aluminium conducting wires (fuse) as well as the positive common plate, and the battery module housing because little heat can be transferred to these parts. Secondly, the heat generation both as the results of heat losses from Joule effect heating and electrochemical reactions of the battery is set at the maximum heat generation of battery [6]. Finally, the cooling system of the battery pack is not considered.

### *3.2 Boundary condition*

The boundary conditions as shown in Fig. 2 are no-slip at battery surfaces, the temperature of cooling air at the inlet side is 25 °C and the air mass flow rate was set to be 0.0175 kg/s. A heat generation model from each single battery cell was used in the simulation.

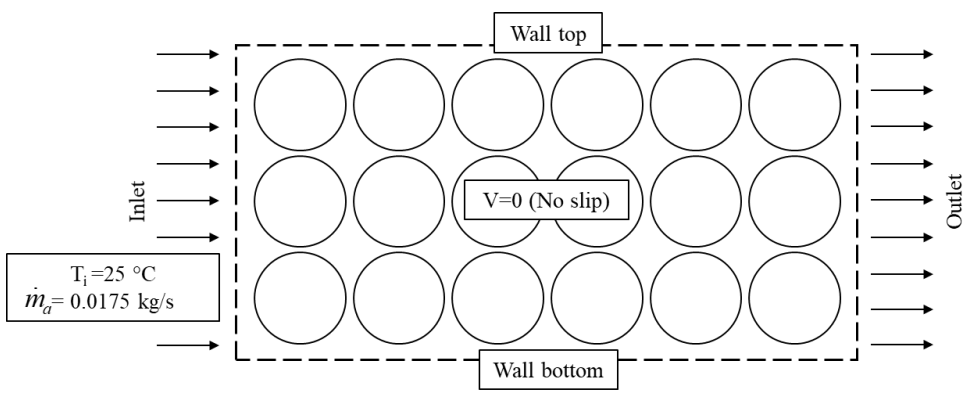


**Fig. 2.** The boundary condition of the 2D battery pack.

### *3.3 Mesh model*

In the 2D battery pack model, a uniform mesh distribution was used with a multizone quad/tri method. For the element size is 0.05 cm. The division of the multizone quad/tri mesh was adopted on the cross-section of the battery module as shown in Fig. 3, the maximum size is 2.55 mm of mesh quality for the simulation model. The designed mesh quality was keeping the minimum orthogonal quality which was greater than 0.1 and lower than 0.95 of maximum skewness. These values were acceptable for the meshing model.

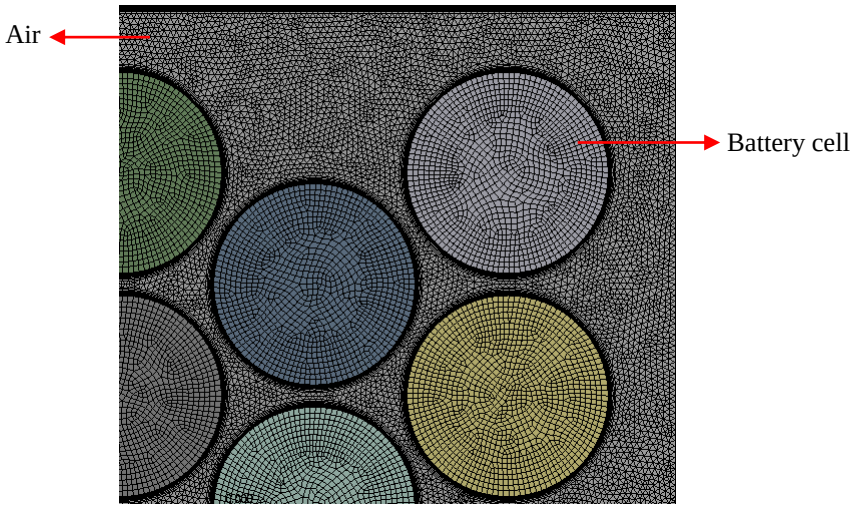


**Fig. 3.** The mesh on the cross-section of the 2D battery pack.

## 4. Results and Discussion

### *4.1 The effect of increasing number of columns on the battery pack using 90° connection*

Figure 4 shows the average temperature of the cells in the aligned arrays. It could be seen from the Fig.4 that increasing numbers of column causes temperature rise at the constant inlet velocity. The maximum temperature of aligned arrays is 28.598 °C. The temperature distribution of cells with 9 columns is the maximum number of columns as shown in Fig. 5. The high temperature occurs at the air outlet side and near the middle of the battery pack, while the temperature of cells near the wall is closest to the ambient temperature. This result can be explained by the fact that the increasing of the number of columns leads to reduce the air velocity and lower the heat dissipation of the battery.

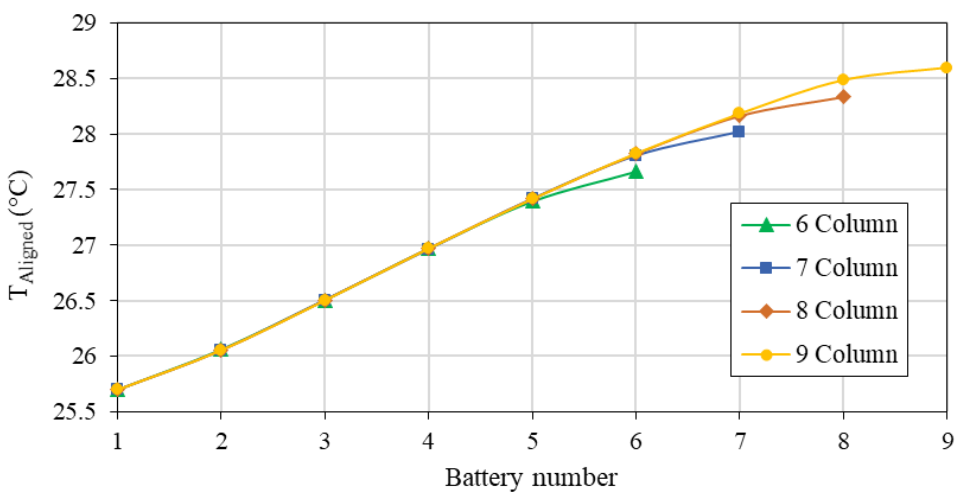


**Fig. 4.** The average temperature of battery pack with different number of columns in aligned arrangement.

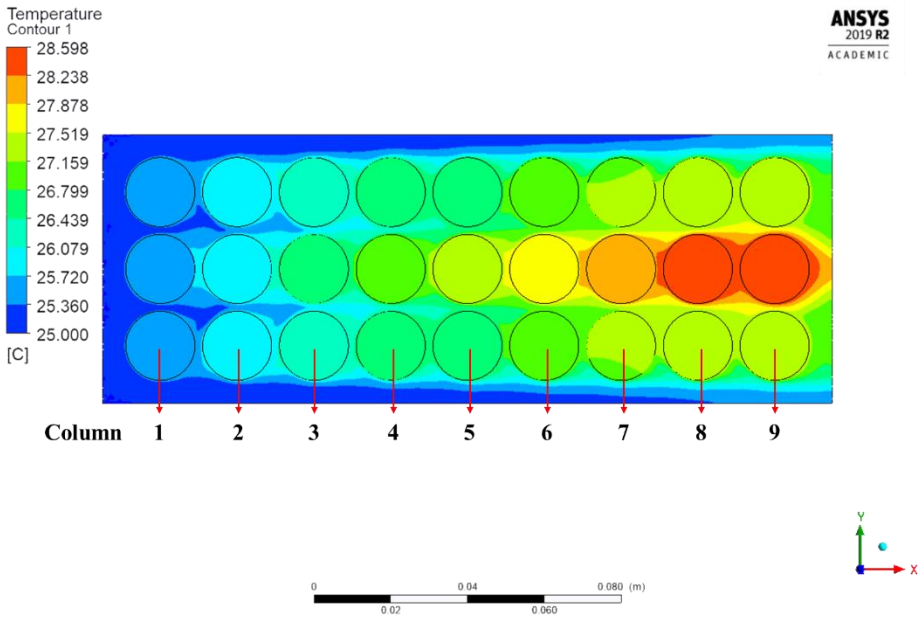


**Fig. 5.** The temperature distribution of battery pack with 9 columns in aligned arrangement.

*4.2 The effect of increasing number of columns on the battery pack using 60° connection*

Figure 6 shows the average temperatures of the cells in the staggered arrangement with an increasing number of columns. The temperature of the staggered arrangement presents different distributions from the aligned arrangement of the battery pack. It can also be seen that the temperature is higher with much of the number of columns is increased. The maximum average temperature for the staggered arrangement is greater than that of the aligned arrangement at the same air mass flow rate because of the staggered structure for air cooling enhancing the local convective heat transfer, which worsens the temperature differences between the cells. The maximum temperature of 9 columns for the staggered arrangement is 29.140 °C as shown in Fig. 7. The high temperature occurs at the air outlet side as well.

From the cell arrangement modes, the aligned arrangement has the best cooling effectiveness and temperature uniformity. However, the maximum temperature difference between aligned and staggered was slightly different results.

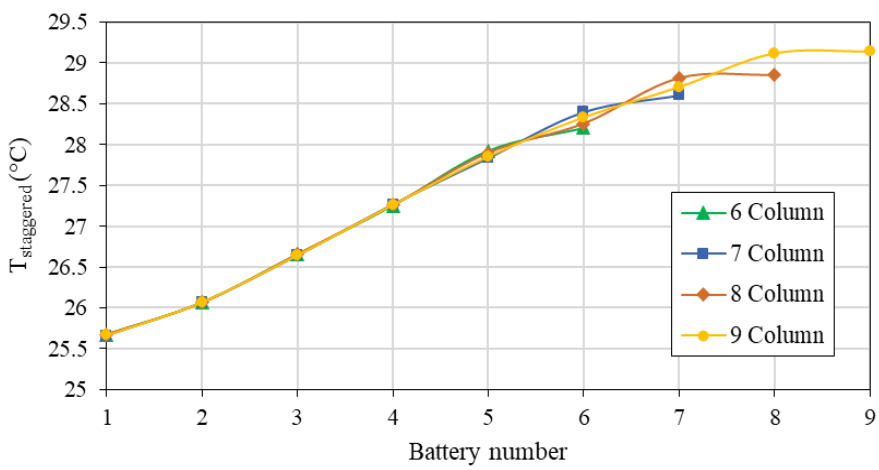


**Fig. 6.** The average temperature of battery pack with different number of columns in staggered arrangement.

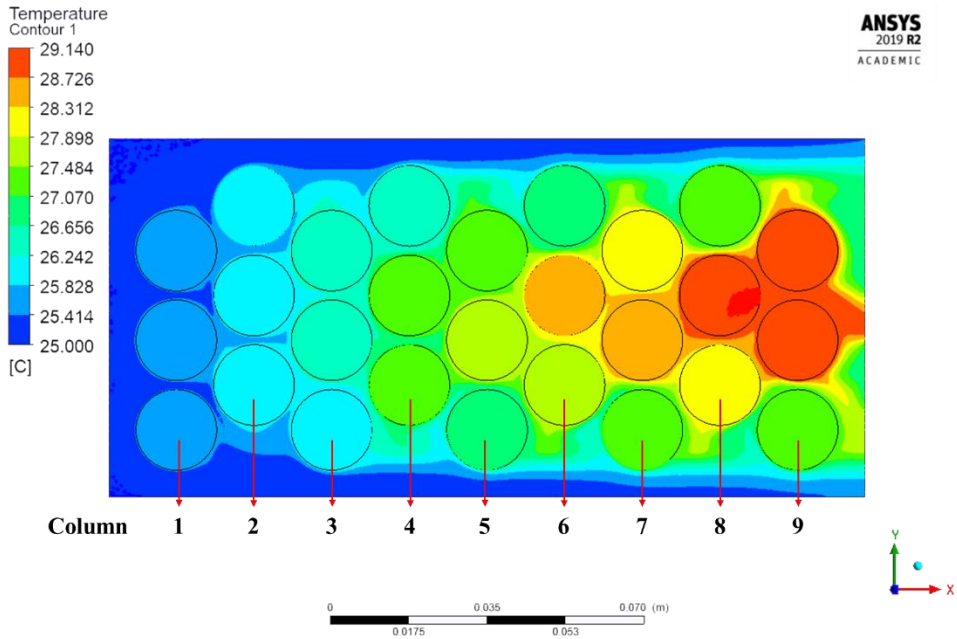


**Fig. 7.** The temperature distribution of battery pack with 9 columns in staggered arrangement.

*4.3 The parametric study of adjusting the gaps between center of battery cells*

The battery pack using 90° connection (aligned) has good cooling effectiveness. However, for practical applications, the free space inside the battery pack cannot be easily accessed manually or even with standard tools when the 90° connection is used [6]. On the other hand, the free space at the side of the battery pack, which uses the 60° connection, can be exploited. For example, for the installation of electronic devices, cables, etc. This is the reason why the space utilization of the 60° connection is better and more complex than that of the 90° connection in practice. Therefore, this section focused on the technique to reduce the temperature of the battery pack by adjusting the gaps between cells from 10 mm of a normal case to other gaps in a staggered arrangement. The parametric study of adjusting the gaps between cells from the center to center (Y) is 11, 12 and 13 mm as shown in Fig. 8.

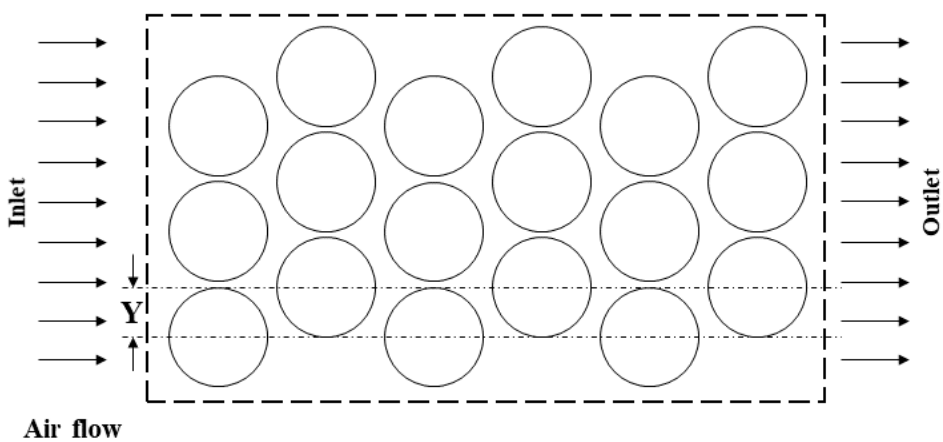


**Fig. 8.** The schematic diagram of the staggered battery pack with adjusting the gaps between cells.

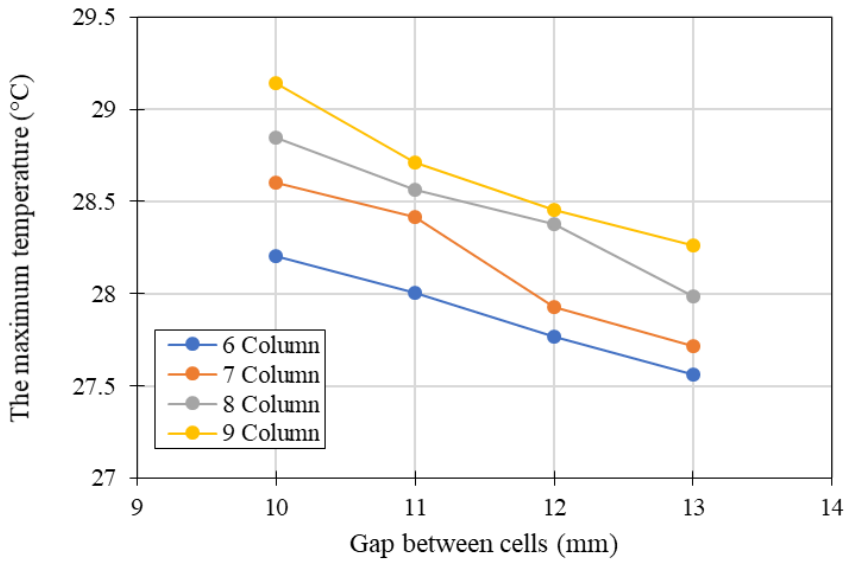


**Fig. 9.** The maximum temperature of battery pack with different gaps between cells in staggered arrangement.

In order to analyze the influence of different gaps between cells on the maximum temperature inside the battery pack. As shown in Fig. 8, the maximum temperature varies with Y under different gaps of the battery cells. It could be seen from Fig. 9 that the maximum temperature of the battery pack continues to decrease with the increasing Y because when increase Y leads to improve the turbulent flow of air which has a larger heat transfer. This study found that the gap between cells at 13 mm is the best option for the design of the battery pack.

## 5. CONCLUSION

### *5.1 The effect of increasing number of columns on the battery pack*

The aligned arrangement has the best cooling performance. In contrast, the average temperature of staggered pack was greater than that of the aligned pack at the same air mass flow rate because the temperature differences between the cells of the staggered structure are worsens. However, the maximum temperature difference of aligned and staggered was slightly different.

### *5.2 The parametric study of adjusting the gaps between center of battery cells*

The result found that the gap at 13 mm is the best option in this study. The temperature decreased by increase the gaps between cells due to the gaps between cells lead to improve the turbulent flow which was larger heat transfer. However, the decreasing temperatures after adjusting the gaps between cells were not significant. Thus, a proper air-cooling system was required.

This study just shows the patterns to improve the temperature uniformity of the battery. In future work, this battery configuration will be validated with the experiment simultaneously to find an appropriate gap of the battery pack.

## NOMENCLATURE

| | |
|---|---|
| $A$ | heat transfer surface area, $m^2$ |
| $C$ | C-rate (Discharge rate) |
| $D$ | longitudinal gap, mm |
| $F$ | Faraday's constant, ($9.65 \cdot 10^5$ s·A/mol) |
| $k$ | turbulence kinetic energy |
| $L$ | transverse gap, mm |
| $\dot{m}_a$ | air mass flow rate, kg/s |

| | |
|---|---|
| p | Reynolds-averaged pressure |
| $\dot{Q}_{battery}$ | heat generation of battery, W |
| $\dot{Q}_{joule}$ | Joule heating, W |
| $\dot{Q}_{entropy}$ | heat generation due to entropy change, W |
| $R_{\text{int}}$ | internal resistance, Ω |
| $\Delta s$ | entropy change, J/mol/K |
| $T$ | absolute temperature, Ω |
| $T_i$ | air inlet temperature, °C |
| $Y$ | gap between cells, mm |
| $\mu_t$ | turbulent viscosity |
| ε | dissipation rate |
| $\sigma_k$ | turbulence kinetic energy Prandtl number |
| $\sigma_T$ | turbulence dissipation rate Prandtl number |
| $\rho_a$ | air density |

*Subscripts*

| | |
|---|---|
| a | air |
| i | inlet |
| int | internal |


## ACKNOWLEDGMENTS

This work was supported by The National Metal and Materials Technology Center (MTEC) and King Mongkut's University of Technology Thonburi (KMUTT). The author would like to acknowledge for personal financial support from Thailand Advance Institute of Science and Technology-Tokyo Institute of Technology (TAIST-Tokyo Tech) and Thailand Graduate Institute of Science and Technology Scholarship (Grant No. TG-MT-KMUTT-62-028M). The author also appreciates all my advisors from MTEC and KMUTT for their help with the simulation.


## REFERENCES


[1] Kim, J., Oh, J. and Lee, H. Review on battery thermal management system for electric vehicles, Applied Thermal Engineering, Vol. 149, 2019, pp. 192-212.

[2] Yang, N., Zhang, X., Li, G. and Hua, D. Assessment of the forced air-cooling performance for cylindrical lithium-ion battery packs: A comparative analysis between aligned and staggered cell arrangements, Applied Thermal Engineering, Vol. 80, 2015, pp. 55-65.

[3] Changwei, J., Bing, W., Shuofeng, W., Shuai, P., Du, W., Pengfei, Q., et al. Optimization on uniformity of lithium-ion cylindrical battery module by different arrangement strategy, Applied Thermal Engineering, Vol. 157, 2019, pp. 1225-1233.

[4] Khan, W.A., Culham, J.R. and Yovanovich, M.M. Convection heat transfer from tube banks in crossflow: Analytical approach, International Journal of Heat and Mass Transfer, Vol. 49, 2006, pp. 4831-4838.

[5] Žukauskas, A. Heat transfer from tubes in crossflow, Advances in Heat Transfer, Vol. 18, 1987, pp. 87-159.

[6] Haider, M., Danish, S., Khan, W., Mehdi, S. and Abbasi, B. Heat transfer and fluid flow over circular cylinders in cross flow, NUST Journal of Engineering Sciences, Vol. 3(1), 2010, pp. 67-77.

[7] Yoo, S., Kwon, H. and Kim, J. A study on heat transfer characteristics for staggered tube banks in cross-flow, Journal of Mechanical Science and Technology, Vol. 21, 2007, pp. 505-512.

[8] Fan, Y., Yun, B., Chen, L., Yanyan, C., Xiaojun, T. and Shuting, Y. Experimental study on the thermal management performance of air cooling for high energy density cylindrical lithium-ion batteries, Applied Thermal Engineering, Vol. 155, 2019, pp. 96-109.

[9] Masomtob, M. A new conceptual design of battery cell with an internal cooling channel: Chapter 3, 2017, RWTH Aachen University, Germany, pp. 20-36.

[10] Chanthevee, P. and Masomtob, M. Thermal performance of cooling system using liquid coolant at cylindrical cell terminal for lithium-ion battery module: Chapter 3, 2018, KMUTT, Thailand, pp. 20-36.

[11] Kowitkulkrai, T., Kaewpradap, A., Hirai, S., Lailuck, V., Rompho, S. and Masomtob, M. Internal resistance computation of a cylindrical lCO battery for heat generation model, IOP Conference Series, Vol. 501, 2019, pp. 12-57.

[12] Seham, S. and Martin, A. Experimental and numerical studies on air cooling and temperature uniformity in a battery pack, Journal of Energy Research, Vol. 42, 2018, pp. 2246-2262.
[13] Kai, C., Weixiong, W., Fang, Y., Lin, Chen. and Shuangfeng, W. Cooling efficiency improvement of air-cooled battery thermal management system through designing the flow pattern, Energy, Vol. 167, 2019, pp. 781-790.